European Journal of Medicinal Chemistry 132 (2017) 1–10

Contents lists available at ScienceDirect

European Journal of Medicinal Chemistry

journal homepage: http://www.elsevier.com/locate/ejmech

Research paper

Dual-tail approach to discovery of novel carbonic anhydrase IX inhibitors by simultaneously matching the hydrophobic and hydrophilic halves of the active site

Zhuang Hou [a, 1], Bin Lin [a, 1], Yu Bao [b], Hai-ning Yan [a], Miao Zhang [a], Xiao-wei Chang [a], Xin-xin Zhang [a], Zi-jie Wang [a], Gao-fei Wei [a], Mao-sheng Cheng [a], Yang Liu [a, *], Chun Guo [a, **]

[a] Key Laboratory of Structure-Based Drugs Design and Discovery (Ministry of Education), School of Pharmaceutical Engineering, Shenyang Pharmaceutical University, Shenyang 110016 China
[b] School of Life Sciences and Biopharmaceutics, Shenyang Pharmaceutical University, Shenyang 110016, China

ARTICLE INFO

Article history:
Received 21 December 2016
Received in revised form
4 February 2017
Accepted 14 March 2017
Available online 16 March 2017

Keywords:
Carbonic anhydrase
CA inhibitors
Dual-tail approach
Hydrophilic half
Hydrophobic half

ABSTRACT

Dual-tail approach was employed to design novel Carbonic Anhydrase (CA) IX inhibitors by simultaneously matching the hydrophobic and hydrophilic halves of the active site, which also contains a zinc ion as part of the catalytic center. The classic sulfanilamide moiety was used as the zinc binding group. An amino glucosamine fragment was chosen as the hydrophilic part and a cinnamamide fragment as the hydrophobic part in order to draw favorable interactions with the corresponding halves of the active site. In comparison with sulfanilamide which is largely devoid of the hydrophilic and hydrophobic interactions with the two halves of the active site, the compounds so designed and synthesized in this study showed 1000-fold improvement in binding affinity. Most of the compounds inhibited the CA effectively with IC_{50} values in the range of 7–152 nM. Compound **14e** (IC_{50}: 7 nM) was more effective than the reference drug acetazolamide (IC_{50}: 30 nM). The results proved that the dual-tail approach to simultaneously matching the hydrophobic and hydrophilic halves of the active site by linking hydrophobic and hydrophilic fragments was useful for designing novel CA inhibitors. The effectiveness of those compounds was elucidated by both the experimental data and molecular docking simulations. This work laid a solid foundation for further development of novel CA IX inhibitors for cancer treatment.

© 2017 Elsevier Masson SAS. All rights reserved.

1. Introduction

The carbonic anhydrases (CAs) form a family of metalloenzymes playing an important role in many physiological processes of prokaryotes and eukaryotes [1]. They catalyze the reversible hydration process of carbon dioxide to bicarbonate and proton [2]. So they are also known as carbonate dehydratases. The family of human carbonic anhydrases (hCAs, EC 4.2.1.1) comprises 16 different α-carbonic anhydrase isoforms [3], including several cytosolic isoforms (CA I~III, CA VII and CA XIII), five membrane-bound isoforms (CA IV, CA IX, CA XII, CA XIV and CA XV), two mitochondrial isoforms (CA VA and CA VB), and one secreted into saliva (CA VI) [4–6]. The hCAs are involved in various biological processes, such as gluconeogenesis, lipogenesis and ureagenesis.

Recently, tumor-associated membrane CA isoform (CA IX) has drawn much attention [7]. Many reports are published studying the roles of CA IX in tumor physiology, such as the control of tumor pH and influence on other processes in the cell microenvironment that promote cell proliferation, invasion, or metastasis [8]. The expression of CA IX is remarkably up-regulated via the hypoxia inducible factor-1 (HIF-1) transcription factor [9]. The over-expression of CA IX will induce the pH imbalance in tumor tissue, and contribute significantly to the extracellular acidification of solid tumors. Thus, CA IX has been a promising target for hypoxic tumor treatment [10–12].

Many efforts have been made for the development of CA inhibitors (CAIs) in hopes of therapeutic cancer treatment. Some

* Corresponding author.
** Corresponding author.
E-mail addresses: y.liu@syphu.edu.cn (Y. Liu), gc_66888@163.com (C. Guo).
[1] These two authors contributed equally to this work.

http://dx.doi.org/10.1016/j.ejmech.2017.03.023
0223-5234/© 2017 Elsevier Masson SAS. All rights reserved.

remarkable results have been achieved since the introduction of the tail approach [13,14]. In this approach, "tails" are appended to the scaffolds of aromatic/heterocyclic sulfonamides possessing derivatizable moieties of the amino, imino or hydroxy type, in such a way that an elongated molecule is obtained with its tail able to interact with amino acid residues from the middle and edge of the active site cavity [15]. Traditionally, most of the "tails" are hydrophobic moieties. Lately, glycosyl moieties were incorporated into different CAI scaffolds as the hydrophilic kind of "tails". Such an approach was also termed "sugar approach", which has led to the development of numerous potent inhibitors of potential clinical use [16–18]. Based on the analyses of the numerous crystallographic structures of CAII and CA IX, it was revealed that the CA active site cavity can be partitioned into two conserved subpockets, one of which comprises a lining of hydrophobic amino acids while the other comprises mainly hydrophilic amino acids [4,19]. Traditionally, the tail approach was utilized to fill the hydrophobic subpocket whereas the sugar approach was utilized to fill the hydrophilic subpocket. Neither approach was able to fill both the subpockets. It is not surprising then that all of the clinically used CAIs so far exhibit broad CA isozyme inhibition due to lack of specificity and their use is associated with side effects. Tanpure et al. attempted to improve the specificity with dual-tail moieties to match both the hydrophobic and hydrophilic halves of the CA active site [20]. However, the compound with one hydrophobic tail and one hydrophilic tail designed by the dual-tail approach has less inhibitory activity than the reference compound acetazolamide (AAZ), even though both single-tail compounds have substantially improved inhibition compared to AAZ. One likely reason is that the relative positions of the two tails are not optimal for synergetic effects.

In this study, the same dual-tail approach was employed to design novel CAIs by choosing an amino glucosamine fragment as the hydrophilic part and a cinnamamide fragment as the hydrophobic part. The cinnamamide fragment was attached to the glucosamine moiety by design to draw optimal interactions with the active site cavity. The inhibitory activities for those compounds confirmed the validity of the dual-tail approach, showing that single-tail compound has moderate improvement and dual-tail compounds have substantial improvement compared to the reference compound sulfanilamide. Molecular docking simulations were performed to elucidate the modes of binding for those compounds.

2. Results and discussion

2.1. Dual-tail approach to compound design

It was long known that sulfonamides and their isosteres (sulfamates/sulfamides) constitute the main class of CAIs due to their effective binding to the zinc metal ion within the enzyme active site [21]. Other zinc-binding motifs also have emerged as new classes of compounds that inhibit CAs from human or from bacterial and fungal pathogens, such as dithiocarbamates and their derivatives, hydroxamic acid and salicylaldoxime [22,23]. An aromatic ring is usually attached directly to those the zinc-bing groups. Such a strategy is also termed the ring approach. Most clinically used CAIs are examples of this approach. The tail approach is another strategy to further develop CAIs. In the tail approach, the aromatic sulfonamide ring incorporates further substitution with tail moieties that are selected to modulate interactions with the active site cavity. If the tail is a flexible hydrophobic group, it will generally adopt a conformation to interact with the hydrophobic half of the CA active site. Likewise, a flexible hydrophilic tail will generally interact with the hydrophilic half of the active site. Traditionally, when developing CAIs, either a hydrophobic tail or a hydrophilic tail was introduced. Dual-tail approach was introduced by Tanpure et al. when they appended a phenyl moiety as the hydrophobic tail and a glucosyl moiety as the hydrophilic tail. However, such a compound was shown to have less inhibitory activity than the reference compound acetazolamide. In this study, we revisited the dual-tail approach by choosing different tails and more importantly, different ways to connect both tails to each other. The cinnamic acid moiety was chosen as the hydrophobic tail because it was found to be a novel structural motif for CA inhibition by Maresca et al. [24]. An amino glucosamine moiety was chosen as the hydrophilic tail because it was found to be active as CAIs in our laboratory (unpublished results). The approach is illustrated in Fig. 1. Nine target compounds were designed by this approach (Table 1). The CA inhibition tests confirmed that those compounds were significantly more active in both CA II inhibition and CA IX inhibition.

2.2. Chemistry

The general synthetic strategies for the formation of the target compounds are shown in Scheme 1 and Scheme 2. D-Glucosamine hydrochloride was selected as the starting material. Intermediate **3** was synthesized *via* selective protection of the primary amino using a Troc protecting group, followed by acetylation with acetic anhydride in pyridine. Next, the glycosyl bromide **4** was prepared by the reaction of **3** with HBr−AcOH in good yield.

The formation of **5** was achieved after activation of α-bromide, using silver carbonate in CH_3OH by the classical Koenigs−Knorr-reaction reaction [25]. Then the addition of zinc to a solution of **5** in acetic acid resulted in the selective removal of the Troc group. Condensation of **6** with substituted cinnamoyl chloride followed by deacetylation with a catalytic amount of $NaOCH_3$ in CH_3OH gave the target analog **8** [26].

As presented in Scheme 2, the starting compound **4** could be readily converted to **9** with NH_4SCN in the mixture of acetone and acetonitrile (1:1). The subsequent treatment of **9** with sulfonamide in the presence of pyridine led to the formation of **10** in 98% yield. Then, the addition of zinc powder to a solution of **10** in acetic acid resulted in the selective removal of the Troc group. The *O*-acetate of **11** was subsequently removed by catalytic amount of $NaOCH_3$ in CH_3OH to liberate the fully deprotected sugar analog **12**. Condensation of **11** with substituted cinnamoyl chloride followed by deacetylation with a catalytic amount of $NaOCH_3$ in CH_3OH gave the target analogues **14a-14g**.

2.3. Biological activity

2.3.1. CA inhibition studies

The CA inhibitory profile of all the newly synthesized compounds and the reference compounds acetazolamide (AAZ) and sulfanilamide (SA) have been investigated for the inhibition of cytosolic, ubiquitous isozymes hCA II as well as membrane associated isozymes hCA IX. The results are shown in Table 1.

The cytosolic isoform hCA II and hCA IX are not at all inhibited by *p*-methoxycinnamic acid (IC_{50} > 100 μM) and are only weakly inhibited by SA (IC_{50} ~ 10 μM). Because both compounds are the parts of compounds designed by the dual-tail approach, it shows that individual components are not active in hCA inhibition. Compound **8**, which is condensed from an amino glucoamine and a *p*-methoxycinnamic acid, has better but still very poor inhibitory activity against the two hCAs (IC_{50} ~ 10 μM). This is not surprising considering that there is no zinc binding group in this compound. However, the inhibitory activity increases into nanomolar range for compound **12**, which is a condensation between an amino glucoamine and SA via a thiourea linker. It shows that SA is very important as a zinc binding group when designing CAIs, consistent

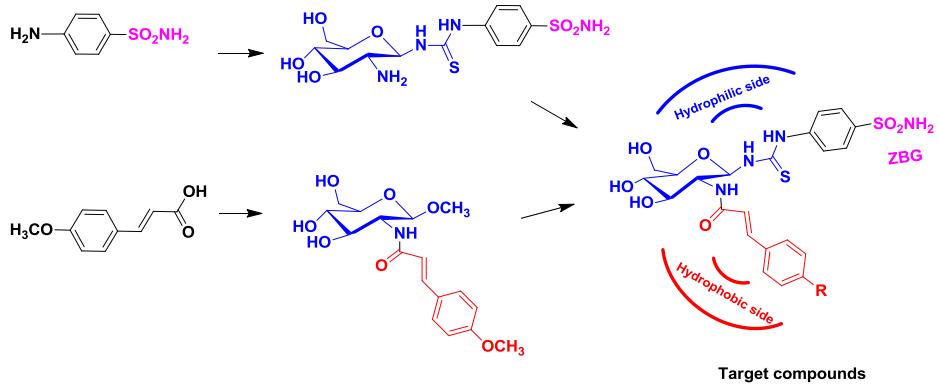

Fig. 1. Dual-tail approach to designing CAIs by attaching an amino glucosamine group as the hydrophilic fragment via a thiourea linker to a sulfanilamide as the zinc binding group (ZBG) then attaching a cinnamamide group to the glucosyl moiety as the hydrophobic fragment.

Table 1
The inhibitory activities of the compounds against hCA II and hCA IX.

Compounds	Structure	IC_{50} (μM)[a,b]	IC_{50} (μM)[a,b]
	R	hCA II	hCA IX
p-methoxycinnamic acid	–	760	850
SA	–	7.5	12
8	–	14	20
12	–	0.203	0.667
14a	4-OCH_3	0.065	0.152
14b	3-OCH_3	0.045	0.095
14c	2-OCH_3	0.053	0.060
14d	2,3-OCH_3	0.034	0.033
14e	2,4-OCH_3	0.025	0.007
14f	2,4,5-OCH_3	0.063	0.037
14g	3,4,5-OCH_3	0.055	0.046
AAZ	–	0.013	0.030

[a] Human recombinant enzymes, by the esterase assay (4-nitrophenylacetate as substrate).
[b] Relative errors were in the range of 5–10% of the reported values, calculated from three independent assays.

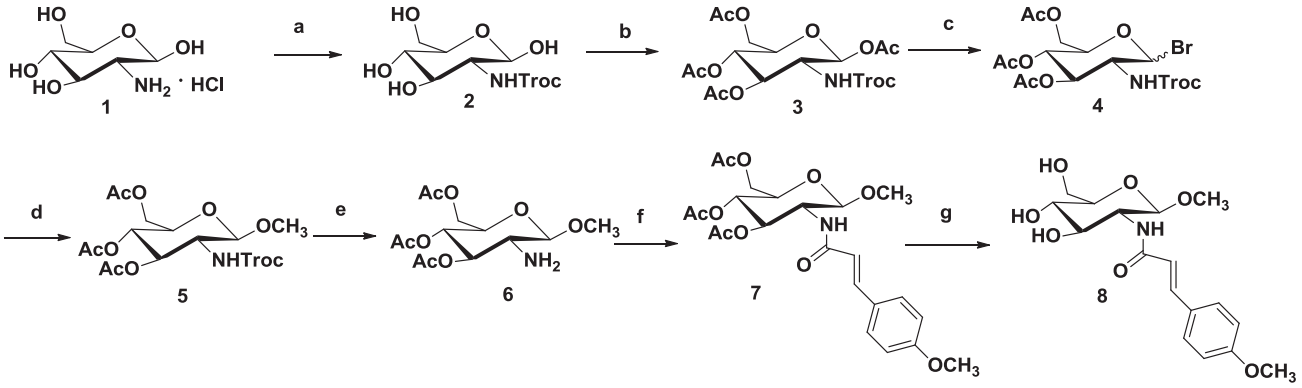

Reagents and conditions: (a) Troc-Cl, $NaHCO_3$, H_2O, r.t., 5 h, 95%; (b) Ac_2O, pyridine, 5 h; (c) HBr-AcOH, CH_2Cl_2, r.t., 6h, 62% (two steps); (d) Ag_2CO_3, CH_3OH, 1 h, 85%; (e) Zinc dust, glacial AcOH r.t., 2h, 96%; (f) Pyridine, DCM, 0°C- r.t., 3h; (g) NaOMe, MeOH, r.t., 85% (two steps).

Scheme 1. Synthesis of compound **8.**

with numerous previous findings in literature. It also shows the importance of the hydrophilic glucosyl moiety. The combination of both designed by the single-tail approach increases the inhibitory activity by an order of magnitude, presumably due to simultaneously binding to the zinc ion and occupying the hydrophilic subpocket of the active site. When the dual-tail approach is applied, compounds **14a-14g** show significant increase in the inhibitory activity, improved by another order of magnitude compared to compound **12**. This put those compounds on a par with AAZ, which is considered the par excellence CA inhibitor and is approved for the treatment of a range of conditions including glaucoma, epilepsy, and altitude sickness. Notably, compound **14e** is even much better than AAZ for hCA IX inhibition (IC_{50} 7 nM vs 30 nM). This is presumably due to the simultaneously matching the hydrophilic

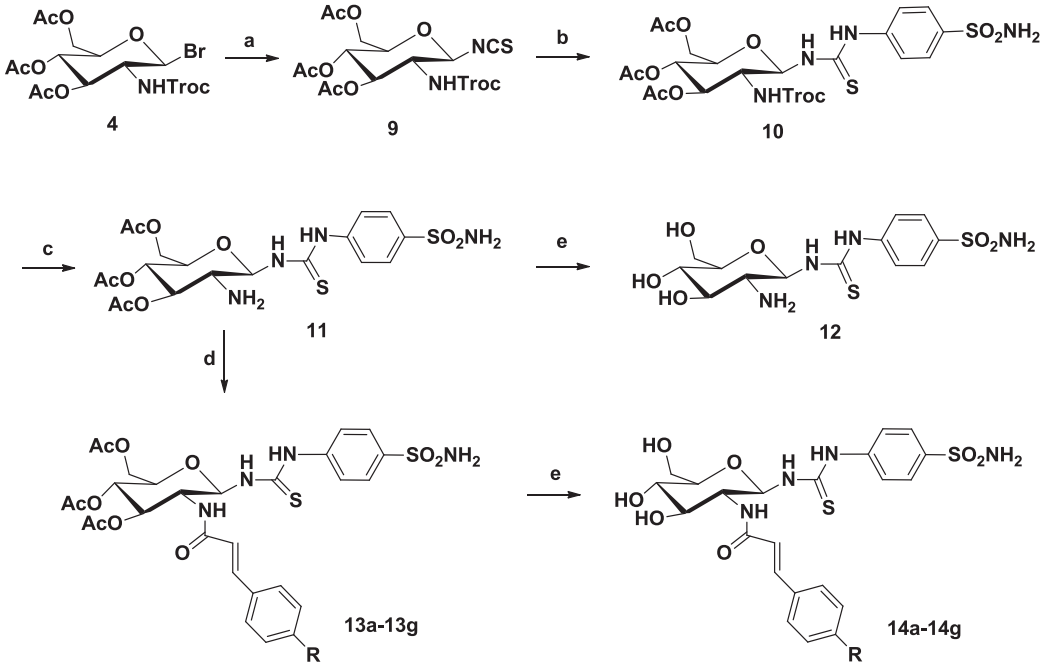

Reagents and conditions: (a) NH_4CNS, acetonitrile, 85°C, 3 h, 55%; (b) Pyridine, 1 h, 98%; (c) Zinc dust, glacial AcOH, r.t., 2 h, 90%; (d) Pyridine, DCM, 0°C- r.t., 3 h; (e) NaOMe/MeOH, r.t.

Scheme 2. Synthesis of compounds **12, 14a-14g.**

half of the active site with the hydrophilic glucosyl moiety and the hydrophobic half with the cinnamamide moiety, in addition to the sulfonamide as the zinc binding group. The modes of binding will be analyzed in detail in the docking analysis section.

2.3.2. Antitumor assay and MTT assay

To assess the antitumor ability and the ability to inhibiting the metabolic activity of those compounds on the cellular level, two cellular models, namely, the colon carcinoma HT-29 and the breast cancer MDA-MB-231 cell models were selected. Cells were grown subconfluent in 96-well plates under normal conditions (37 °C, 5% CO_2 in air), with half of the plates from each cell line incubated under normal conditions (normoxia) and the other half subjected to hypoxic conditions (1% O_2, 5% CO_2 and 94% N_2) to induce the expression of CA IX [27–29].

Compounds **14a-14g** were evaluated on their *in vitro* growth inhibitory activities against colon cancer cell lines that overexpress a high amount of CA IX under normoxic conditions. We compared the effects of compounds **14a-14g** with those of the standard sulfonamide inhibitor AAZ under the same conditions. AAZ did not show any activity in these *ex vivo* assays as suggested by the uncompromised cell viability. However, reduced cell viability was observed for compounds **14a-14g** after 72 h incubation under both normoxia and hypoxia conditions for both cancer cell lines (see Fig. 2).

As shown in Fig. 2, all the compounds were able to reduce tumor cell viability in both cancer cell lines, with a greater impact elicited in hypoxic conditions where CA IX is generally overexpressed. Colon HT-29 cancer cell (73–79% cell viability) was slightly more sensitive to the exposure of those compounds than breast MDA-MB-231 cancer cell (89–99% cell viability) in normoxia while much more sensitive in hypoxia (63%–77% cell viability for HT-29

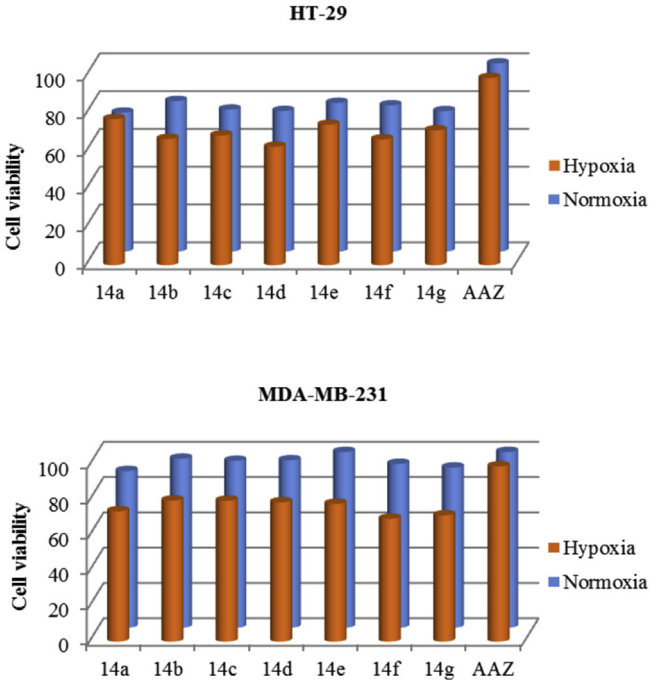

Fig. 2. Effects of compouds **14a-14g** and acetazolamide, at 100 μM concentration, on the viability of colon HT-29, breast MDA-MB-231 cell lines under normoxic and hypoxic conditions. Values are the average of three independent experiments. Relative errors are generally within 5–10%.

and 69.5%–79.9% cell viability for MDA-MB-231). It is worth noting that even though AAZ has excellent inhibitory activity against both CA II and CA IX enzymes, it has almost no activity against the cancer cell lines investigated in this study. This is in sharp contrast with the compounds designed by the dual-tail approach as CAIs, which showed good inhibitory activities both at the enzyme level and at the cellular level.

On the other hand, compound **14e** does not show the best antitumor activity among the test compounds, although it is the highest one in CA IX inhibition assay. This indicates that CA IX is merely one of tumor-associated targets and CA IX inhibitors are not potent enough to be used alone in cancer therapy.

2.3.3. *Inhibition of extracellular acidification in cancer cells by compound **14e***

CA IX is functionally linked to the control of tumor pH [30–32], and hypoxia-induced extracellular acidosis is a measure of the biological activity of CA IX in cultured cells [33]. MDA-MB-231 demonstrated increased CA IX expression upon hypoxia, while HT-29 also had a high expression under ambient air [34]. Therefore, we tested the compound **14e** for its effect on pH in hypoxia and normoxic conditions. We found sulfonamide **14e** was able to reduce the extracellular acidification of cancer cells in 0.1 and 1 mM concentrations (Fig. 3). This compound resulted in a significant reduction in hypoxia-induced extracellular acidosis, while the effect on cells exposed to ambient air was weak. Furthermore, a dose-dependent effect was observed.

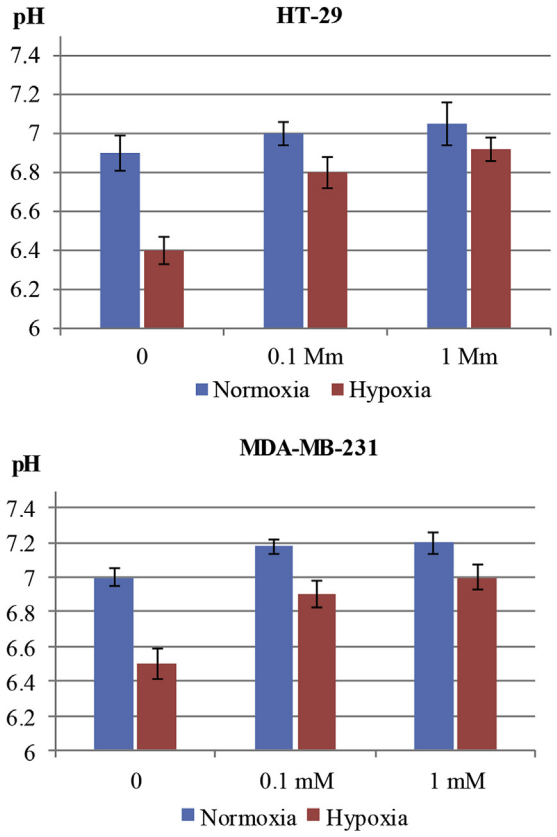

Fig. 3. Inhibition of extracellular acidification of HT-29 and MDA-MB-231 cancer cells in normoxia and hypoxia upon treatment with compound **14e** (0.1 and 1 mM). The pH values were measured after 48 h. Three independent experiments with three parallel dishes per sample were performed.

3. Molecular docking analyses

Molecular docking studies started with a redocking experiment by AutoDock 4.2.6 with the AutoDock4Zn force field for AAZ with CA IX (PDB: 3IAI). The redocking results showed that the crystal pose of AAZ was reproduced fairly well, especially with the interactions between the sulfonamide functional group of AAZ and the zinc ion in CA IX. This is the characteristic of sulfonamides as CAIs, which the compounds in Table 1 will follow. Next, the same model was applied to the compounds listed in Table 1. The molecular docking results showed the cinnamamide segment of compound **8** to be closely integrated with the hydrophobic region of the CA active site cavity (Fig. 4). The "carbohydrate tail" region of **8** interacts primarily with the hydrophilic pocket of the enzyme, especially with the nitrogen of the imidazole ring of H64.

The molecular docking results showed that sulfonamide can bind to the Zn^{2+} ion and the "carbohydrate tail" region interacts primarily with the hydrophilic pocket of the enzyme on the nitrogen of the imidazole ring of H64 (Fig. 5).

Once again, the molecular docking results showed that the sulfonamide amine N atom of **14e** binds directly to the active-site Zn atom along with the side chains of HIS94, HIS96 and HIS119. The sulfonamide group forms a hydrogen bond to THR199. Furthermore, the guanidino nitrogen atom forms a hydrogen bond to PRO201, and the two oxygen atoms of the glucosyl hydroxy group form hydrogen bonds to SER201 and HIS64 respectively (Fig. 6). The cinnamamide segment of compound **14e** could interact closely with the hydrophobic region of the CA active site cavity. All of molecular docking results showed the flexible hydrophobic tail of **14e** allowed it to interact better with the resides in the hydrophobic pocket of carbonic anhydrase and this in turn helped to stabilize the inhibitor leading to tighter binding compared to **8** and **12**. Therefore, multiple interactions are applied between the compound and the enzyme.

4. Conclusion

A dual-tail approach was applied to improve the affinity of CA inhibitors by accessing additional hydrophobic and hydrophilic interactions on CA active sites. A series of compounds were designed and synthesized to test the validity of this approach. The biological activity studies showed these compounds exhibited inhibitory activity with 1000-fold of the initial fragment SA. Furthermore, the antitumor activity of these compounds was also evaluated under two different conditions. Compared to reference drug acetazolamide, these compounds show increasing anti-proliferation activity. Further studies on their suppressing migration of tumor cells are underway.

5. Experimental section

5.1. Chemistry

Reagents were used without further purification unless otherwise specified. Solvents were dried and redistilled prior to use in the usual way. Analytical TLC was performed using silica gel HF254. Preparative column chromatography was performed using silica gel H. HPLC chromatograms were obtained on a Waters 1525–2489. Melting points were obtained on a Büchi melting point B-540 apparatus. ^{1}H and ^{13}C NMR spectra were recorded on a Bruker ARX 600 MHz spectrometer with TMS as the internal standard. NMR spectra were analyzed and interpreted using MestReNova. ESI-MS spectra were obtained on an Agilent ESI-QTOF instrument. HR-MS were obtained on a Bruker micrOTOF_Q spectrometer.

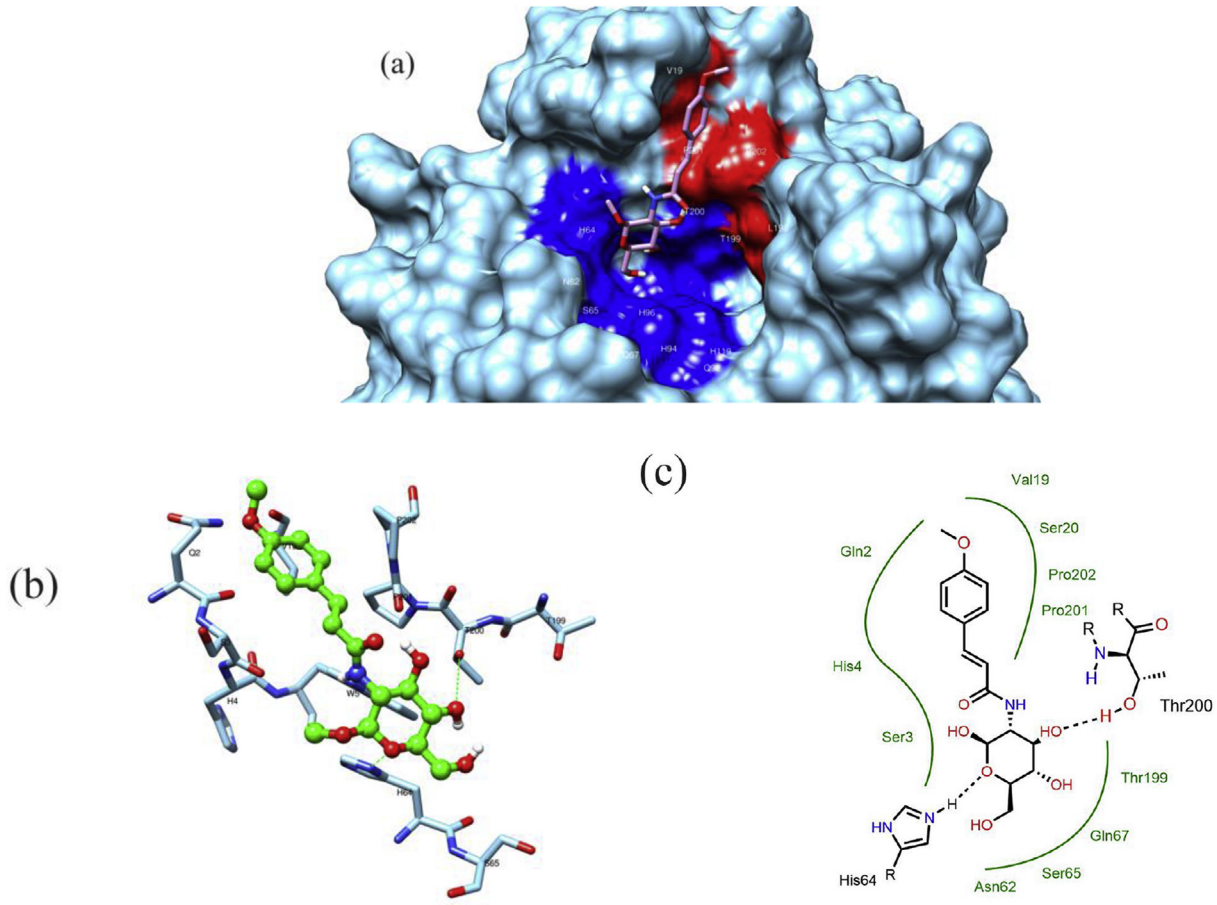

Fig. 4. Interaction diagrams of the selected docked conformations for compound **8** inside the active site of CA IX enzyme. (a) The surface representation of binding pocket has been shown at the top of the figure. (b) 3D ligand interactions diagram has been shown at the left-bottom. Hydrogen bond interactions are shown with dotted lines in green. (c) 2D ligand interactions diagram has been shown at the right-bottom and hydrophobic and hydrophilic interactions are drawn with green lines. (For interpretation of the references to colour in this figure legend, the reader is referred to the web version of this article.)

*5.2. 2-deoxy-2-[[3-(4-methoxylphenyl)-1-oxo-2-propenyl] amino]-β-D-glucopyranose (**8**)*

To a solution of compound **6** (100.0 mg, 0.087 mmol) in dry CH_2Cl_2 (10 mL), substituted cinnamoyl chloride (0.11 mmol) and pyridine (0.2 mL) were added at room temperature and the reaction mixture was stirred for 1 h. The mixture was quenched by addition of MeOH and concentrated. Then, to a solution of residue in CH_2Cl_2-MeOH (1:1, 10 mL), freshly prepared NaOMe in MeOH solution (1.0 mol/L, 1 mL) was added. After it was stirred overnight, the mixture was neutralized with Dowex H^+ resin to pH 7, and then filtered. The filtrate was concentrated and purified by a silica gel column chromatography (10:1, CH_2Cl_2-MeOH) to afford **8** (84.6%) as a white solid. M.p. 115.7–117.2 °C; ^{1} H NMR (600 MHz, DMSO-d_6) δ 7.89 (d, J = 9.1 Hz, 1H), 7.51 (d, J = 8.7 Hz, 2H), 7.35 (d, J = 15.7 Hz, 1H), 6.98 (d, J = 8.7 Hz, 2H), 6.45 (d, J = 15.7 Hz, 1H), 5.01 (d, J = 4.9 Hz, 1H), 4.97 (d, J = 5.6 Hz, 1H), 4.56 (t, J = 6.0 Hz, 1H), 4.26 (d, J = 8.4 Hz, 1H), 3.79 (s, 3H), 3.71 (dd, J = 10.9, 6.1 Hz, 1H), 3.57 (dd, J = 18.7, 9.0 Hz, 1H), 3.48 (dt, J = 11.3, 5.5 Hz, 1H), 3.33 (s, 4H), 3.11 (dd, J = 15.0, 7.1 Hz, 2H). ^{13}C NMR (150 MHz, DMSO-d_6) δ 165.66, 160.72, 138.65, 129.47, 128.01, 120.81, 114.87, 102.39, 77.52, 74.97, 71.17, 61.55, 56.09, 55.81, 55.72. ESI-MS (m/z): 376.4 [M + Na]$^+$; HRMS (ESI): Calcd for [M + Na]$^+$ $C_{17}H_{23}NNaO_7$: 376.1478, Found 376.1459.

*5.3. N-[4-(Aminosulfonyl) phenyl]-N,-(2-amino-2-deoxy-β-D-glucopyranosyl) thiourea (**12**)*

To a solution of **11** (100 mg, 0.19 mmol) in CH_2Cl_2-MeOH (1:1, 10 mL), freshly prepared NaOMe in MeOH solution (1.0 mol/L, 1 mL) was added. After it was stirred overnight, the mixture was neutralized with Dowex H^+ resin to pH 7, and then filtered. The filtrate was concentrated and purified by a silica gel column chromatography (10:1, CH_2Cl_2-MeOH) to afford **12** (64.8 mg, 85.6%) as a white solid. M.p. 155.5–157.1 °C; ^{1} H NMR (600 MHz, DMSO-d_6) δ 11.16 (s, 1H), 9.60 (s, 1H), 7.80 (s, 2H), 7.72 (d, J = 7.6 Hz, 2H), 7.26 (s, 2H), 5.23 (s, 1H), 4.51 (s, 1H), 4.07 (s, 1H), 3.75 (s, 2H), 3.15 (d, J = 16.7 Hz, 4H), 2.63 (s, 1H), 1.84 (s, 2H). ^{13} C NMR (151 MHz, DMSO-d_6) δ 182.55, 143.29, 139.18, 126.45, 122.52, 84.38, 78.90, 77.36, 70.33, 61.22, 56.57. ESI-MS (m/z): 415.1 [M + Na]$^+$; HRMS (ESI): Calcd for [M + Na]$^+$ $C_{13}H_{20}N_4NaO_6S_2$: 415.0828, Found 415.0859.

*5.4. General procedure for the synthesis of compounds (**14a-14g**)*

To a solution of compound **11** (1 equiv) in dry dichloromethane, substituted cinnamoyl chlorides (0.58 equiv) and pyridine were added at room temperature and the reaction mixture was stirred for 1 h. The mixture was quenched by addition of MeOH and concentrated. Then, to a solution of residue in CH_2Cl_2-MeOH (1:1),

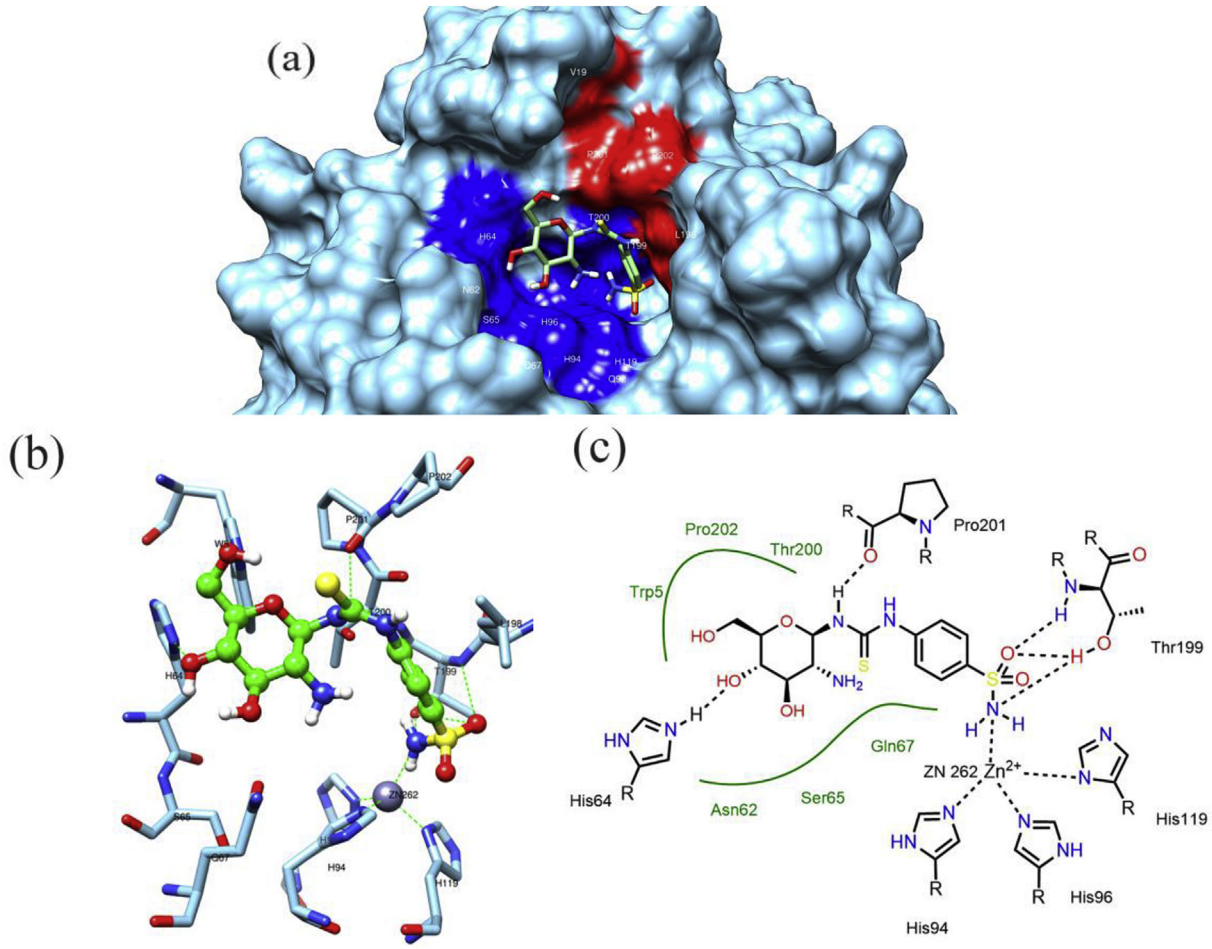

Fig. 5. Interaction diagrams of the selected docked conformations for compound **12** inside the active site of CA IX enzyme. (a) The surface representation of binding pocket has been shown at the top of the figure. (b) 3D ligand interactions diagram has been shown at the left-bottom. Hydrogen bond interactions are shown with dotted lines in green. (c) 2D ligand interactions diagram has been shown at the right-bottom and hydrophobic and hydrophilic interactions are drawn with green lines. (For interpretation of the references to colour in this figure legend, the reader is referred to the web version of this article.)

freshly prepared NaOMe in MeOH solution (1.0 mol/L) was added. After it was stirred overnight, the mixture was neutralized with Dowex H^+ resin to pH 7, and then filtered. The filtrate was concentrated and purified by a silica gel column chromatography (10:1, CH_2Cl_2-MeOH) to afford **14a-14g** (76.8%–92.7%) as a white solid.

*5.4.1. N-[4-(Aminosulfonyl) phenyl]-N,-[2-[(2E)-3-(4-methoxylphenyl)-1-oxo-2-propen-1-yl] amino]-2-deoxy-β-D-glucopyranosyl] thiourea (**14a**)*

M.p. 165.5–167.2 °C; ^{1}H NMR (600 MHz, DMSO-d_6) δ 10.37 (s, 1H), 8.22 (s, 1H), 8.02 (s, 1H), 7.73 (d, J = 8.7 Hz, 2H), 7.69 (d, J = 8.8 Hz, 2H), 7.51 (d, J = 8.4 Hz, 2H), 7.39 (d, J = 15.5 Hz, 1H), 7.27 (s, 2H), 6.98 (d, J = 8.7 Hz, 2H), 6.51 (d, J = 15.8 Hz, 1H), 5.42 (s, 1H), 5.04 (s, 2H), 3.82 (d, J = 9.3 Hz, 1H), 3.78 (s, 3H), 3.65 (d, J = 10.8 Hz, 1H), 3.52 (dd, J = 11.8, 4.5 Hz, 1H), 3.44 (d, J = 7.0 Hz, 2H), 3.23 (dd, J = 17.2, 8.4 Hz, 1H), 3.16 (d, J = 9.9 Hz, 1H). ^{13}C NMR (151 MHz, DMSO-d_6) δ 182.27, 166.86, 160.93, 142.61, 139.68, 139.33, 129.68, 127.75, 126.67, 122.71, 120.08, 114.93, 113.81, 83.75, 78.98, 75.11, 70.78, 61.02, 55.76, 55.41, 54.70. ESI-MS (m/z): 575.4 $[M + Na]^+$; HRMS (ESI): Calcd for $[M + Na]^+$ $C_{23}H_{28}N_4NaO_8S_2$: 575.1251, Found 575.1259.

*5.4.2. N-[4-(Aminosulfonyl) phenyl]-N,-[2-[(2E)-3-(3-methoxylphenyl)-1-oxo-2-propen-1-yl] amino]-2-deoxy-β-D-glucopyranosyl] thiourea (**14b**)*

M.p. 170.9–172.7 °C; ^{1}H NMR (600 MHz, DMSO-d_6) δ 10.38 (s, 1H), 8.33 (d, J = 6.6 Hz, 1H), 8.03 (s, 1H), 7.73 (d, J = 8.9 Hz, 2H), 7.69 (d, J = 8.7 Hz, 2H), 7.41 (d, J = 15.5 Hz, 1H), 7.33 (t, J = 7.9 Hz, 1H), 7.29 (s, 2H), 7.14 (d, J = 7.4 Hz, 1H), 7.12 (s, 1H), 6.97–6.94 (m, 1H), 6.66 (d, J = 15.5 Hz, 1H), 5.43 (s, 1H), 5.10 (s, 2H), 3.83 (d, J = 9.0 Hz, 1H), 3.78 (s, 3H), 3.64 (d, J = 11.0 Hz, 1H), 3.51 (dd, J = 11.8, 4.4 Hz, 1H), 3.44 (dd, J = 14.0, 7.0 Hz, 2H), 3.23 (t, J = 9.1 Hz, 1H), 3.16 (d, J = 8.8 Hz, 1H). ^{13}C NMR (151 MHz, DMSO-d_6) δ 182.25, 166.46, 160.10, 142.60, 139.72, 139.54, 136.65, 130.54, 126.69, 122.98, 122.72, 120.49, 116.01, 113.00, 83.67, 78.99, 75.10, 70.77, 63.58, 61.04, 55.61, 54.78. ESI-MS (m/z): 575.4 $[M + Na]^+$; HRMS (ESI): Calcd for $[M + Na]^+$ $C_{23}H_{28}N_4NaO_8S_2$: 575.1221, Found 575.1241.

*5.4.3. N-[4-(Aminosulfonyl) phenyl]-N,-[2-[(2E)-3-(2-methoxylphenyl)-1-oxo-2-propen-1-yl] amino]-2-deoxy-β-D-glucopyranosyl] thiourea (**14c**)*

M.p. 172.9–174.5 °C; ^{1}H NMR (600 MHz, DMSO-d_6) δ 10.37 (s, 1H), 8.31 (s, 1H), 8.01 (s, 1H), 7.72 (dt, J = 14.0, 8.8 Hz, 5H), 7.52 (d, J = 7.3 Hz, 1H), 7.37 (t, J = 7.8 Hz, 1H), 7.27 (s, 2H), 7.07 (d, J = 8.3 Hz, 1H), 6.99 (t, J = 7.5 Hz, 1H), 6.70 (d, J = 15.7 Hz, 1H), 5.43 (s, 1H), 5.07

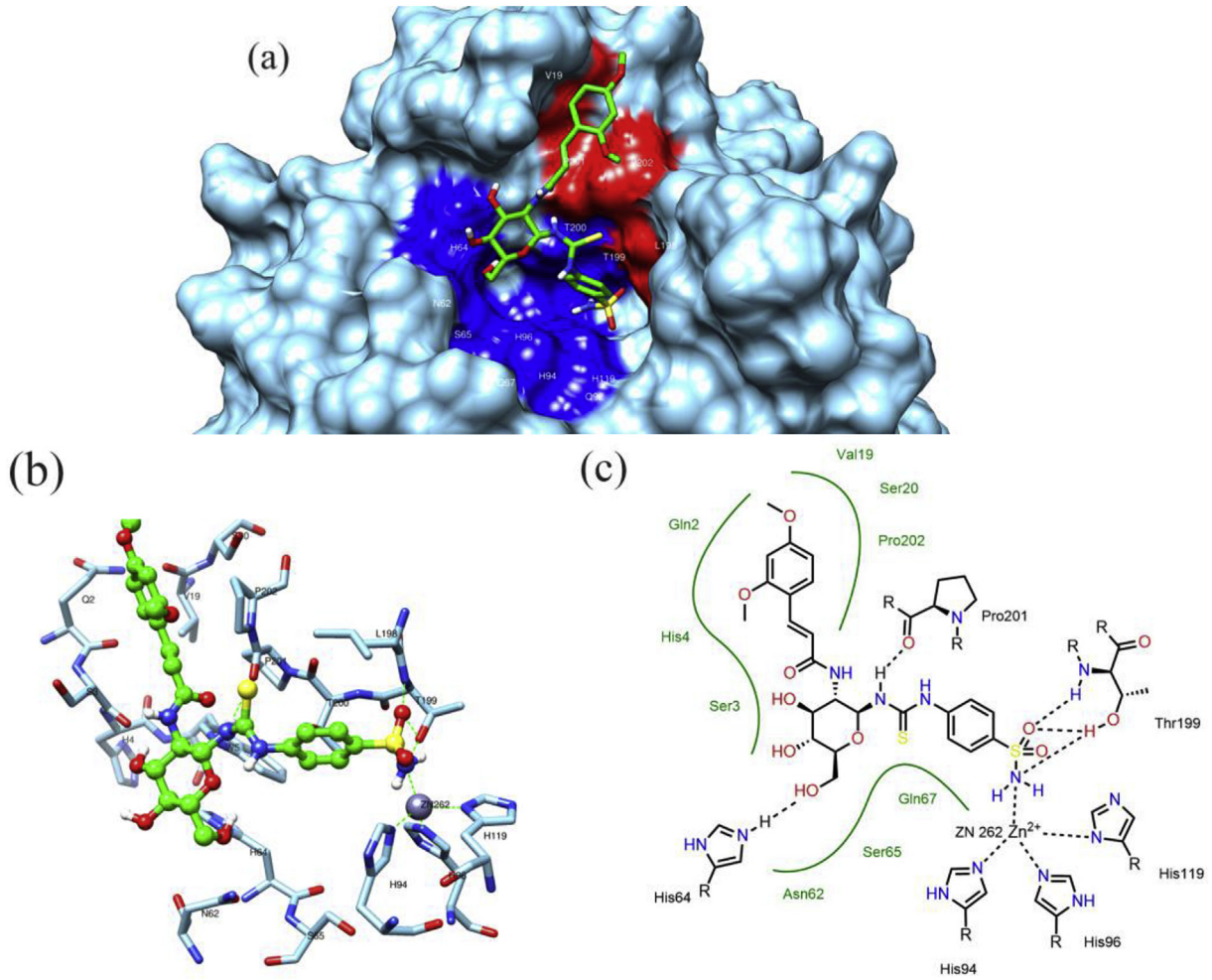

Fig. 6. Interaction diagrams of the selected docked conformations for compound **14e** inside the active site of CA IX enzyme. (a) The surface representation of binding pocket has been shown at the top of the figure. (b) 3D ligand interactions diagram has been shown at the left-bottom. Hydrogen bond interactions are shown with dotted lines in green. (c) 2D ligand interactions diagram has been shown at the right-bottom and hydrophobic and hydrophilic interactions are drawn with green lines. (For interpretation of the references to colour in this figure legend, the reader is referred to the web version of this article.)

(d, J = 20.3 Hz, 2H), 4.52 (s, 1H), 3.85 (s, 3H), 3.65 (s, 1H), 3.55–3.50 (m, 1H), 3.44 (dd, J = 7.0, 5.1 Hz, 2H), 3.24 (dd, J = 14.8, 9.0 Hz, 1H), 3.16 (d, J = 6.6 Hz, 1H). ^{13}C NMR (151 MHz, DMSO-d_6) δ 182.25, 166.96, 158.10, 142.59, 139.67, 134.91, 131.45, 128.60, 126.62, 123.55, 122.78, 121.21, 112.18, 111.00, 83.73, 78.93, 75.03, 70.76, 61.00, 56.05, 55.87, 54.69. ESI-MS (m/z): 575.5 $[M + Na]^+$; HRMS(ESI): Calcd for $[M + Na]^+$ $C_{23}H_{28}N_4NaO_8S_2$: 575.1231, Found 575.1241.

5.4.4. *N-[4-(Aminosulfonyl) phenyl]-N,-[2-[(2E)-3-(2,3-dimethoxylphenyl)-1-oxo-2-propen-1-yl] amino]-2-deoxy-β-D-glucopyranosyl] thiourea (**14d**)*

M.p. 164.6–166.7 °C; ^{1}H NMR (600 MHz, DMSO-d_6) δ 10.41 (s, 1H), 8.37 (d, J = 7.7 Hz, 1H), 8.01 (t, J = 15.3 Hz, 1H), 7.76–7.66 (m, 5H), 7.30 (d, J = 10.1 Hz, 2H), 7.15 (d, J = 7.7 Hz, 1H), 7.11 (t, J = 7.8 Hz, 1H), 7.07 (d, J = 8.0 Hz, 1H), 6.67 (d, J = 15.9 Hz, 1H), 5.43 (s, 1H), 5.10 (s, 2H), 3.90–3.82 (m, 1H), 3.81 (s, 3H), 3.72 (s, 3H), 3.64 (s, 1H), 3.52 (dd, J = 12.0, 4.2 Hz, 1H), 3.46–3.42 (m, 2H), 3.24 (t, J = 9.1 Hz, 1H), 3.17–3.12 (m, 1H). ^{13}C NMR (151 MHz, DMSO-d_6) δ 181.87, 166.28, 152.97, 147.54, 142.26, 139.28, 133.74, 128.41, 126.29, 124.60, 123.27, 122.35, 118.57, 114.04, 83.34, 78.63, 74.71, 70.36, 60.81, 60.61, 60.42, 55.88, 55.77, 54.36. ESI-MS (m/z): 605.4 $[M + Na]^+$; HRMS (ESI): Calcd. For $[M + Na]^+$ $C_{24}H_{30}N_4NaO_9S_2$: 605.1341, Found 605.1349.

5.4.5. *N-[4-(Aminosulfonyl) phenyl]-N,-[2-[(2E)-3-(2,4-dimethoxylphenyl)-1-oxo-2-propen-1-yl] amino]-2-deoxy-β-D-glucopyranosyl] thiourea (**14e**)*

M.p. 148.5–150.2 °C; ^{1}H NMR (600 MHz, DMSO-d_6) δ 10.46 (d, J = 66.9 Hz, 1H), 8.25 (dd, J = 27.8, 7.6 Hz, 1H), 8.03 (s, 1H), 7.83–7.74 (m, 1H), 7.71 (dd, J = 22.9, 8.8 Hz, 4H), 7.61 (d, J = 16.2 Hz, 1H), 7.45 (d, J = 8.4 Hz, 1H), 7.29 (s, 2H), 6.60 (s, 1H), 6.60–6.57 (m, 1H), 5.40 (s, 1H), 5.08 (s, 2H), 4.56 (s, 1H), 3.85 (s, 3H), 3.80 (s, 3H), 3.76 (s, 1H), 3.63 (s, 1H), 3.54–3.49 (m, 2H), 3.23 (dd, J = 16.4, 7.5 Hz, 1H), 3.12 (s, 1H). ^{13}C NMR (151 MHz, DMSO-d_6) δ 182.30, 167.41, 162.37, 159.60, 142.64, 139.68, 134.90, 130.05, 126.68, 122.81, 122.30, 120.29, 116.49, 106.46, 98.99, 83.88, 78.97, 75.09, 70.78, 61.00, 56.18, 55.92, 55.50, 54.63. ESI-MS (m/z): 605.4 $[M + Na]^+$; HRMS (ESI): Calcd for $[M + Na]^+$ $C_{24}H_{30}N_4NaO_9S_2$: 605.1339, Found 605.1346.

5.4.6. *N-[4-(Aminosulfonyl) phenyl]-N,-[2-[(2E)-3-(2,4,5-trimethoxylphenyl)-1-oxo-2-propen-1-yl] amino]-2-deoxy-β-D-glucopyranosyl] thiourea (**14f**)*

M.p. 164.4–167.2 °C; ^{1}H NMR (600 MHz, DMSO-d_6) δ 10.40 (s, 1H), 8.19 (s, 1H), 8.02 (s, 1H), 7.73 (d, J = 8.6 Hz, 2H), 7.69 (d, J = 8.7 Hz, 2H), 7.65 (d, J = 15.8 Hz, 1H), 7.29 (s, 2H), 7.07 (s, 1H), 6.71 (s, 1H), 6.57 (d, J = 15.8 Hz, 1H), 5.39 (s, 1H), 5.08 (s, 2H), 4.55 (s, 1H),

3.84 (s, 3H), 3.83 (s, 3H), 3.78 (d, J = 11.5 Hz, 1H), 3.74 (s, 3H), 3.54–3.49 (m, 1H), 3.44 (qd, J = 7.0, 5.1 Hz, 2H), 3.23 (dd, J = 14.7, 8.8 Hz, 1H), 3.14 (s, 1H). ^{13} C NMR (151 MHz, DMSO-d_6) δ 182.30, 167.44, 153.52, 151.91, 143.41, 126.64, 122.83, 114.92, 111.47, 98.51, 83.84, 78.89, 75.03, 70.87, 61.10, 56.84, 56.55, 56.31. ESI-MS (m/z): 635.4 $[M + Na]^+$; HRMS(ESI): Calcd for $[M + Na]^+$ $C_{25}H_{32}N_4O_{10}S_2Na$: 635.1441, Found 635.1454.

5.4.7. N-[4-(Aminosulfonyl) phenyl]-N,-[2-[(2E)-3-(3,4,5-trimethoxylphenyl)-1-oxo-2-propen-1-yl] amino]-2-deoxy-β-D-glucopyranosyl] thiourea (**14g**)

M.p. 207.4–210.6 °C; ^{1} H NMR (600 MHz, DMSO-d_6) δ 10.35 (s, 1H), 8.25 (s, 1H), 8.03 (s, 1H), 7.73 (d, J = 8.7 Hz, 2H), 7.69 (d, J = 8.8 Hz, 2H), 7.38 (d, J = 15.6 Hz, 1H), 7.27 (s, 2H), 6.90 (s, 2H), 6.61 (d, J = 15.5 Hz, 1H), 5.41 (s, 1H), 5.06 (d, J = 16.4 Hz, 2H), 4.52 (s, 1H), 3.81 (s, 7H), 3.68 (s, 3H), 3.67–3.63 (m, 1H), 3.54–3.50 (m, 1H), 3.44 (d, J = 6.8 Hz, 1H), 3.25–3.21 (m, 1H), 3.17 (s, 1H). ^{13} C NMR (151 MHz, DMSO-d_6) δ 182.24, 166.54, 153.57, 142.56, 139.67, 139.21, 130.83, 126.70, 122.65, 122.04, 105.43, 83.69, 78.97, 75.11, 70.77, 61.01, 60.57, 56.34, 54.69. ESI-MS (m/z): 635.5 $[M + Na]^+$; HRMS (ESI): Calcd for $[M + Na]^+$ $C_{25}H_{32}N_4O_{10}S_2Na$: 635.1441, Found 635.1452.

5.5. CA inhibition

Both CA isoenzyme activities were determined according to the method described previously by Verpoorte et al. (1967) [35]. Initial rates of 4-nitrophenyl acetate hydrolysis catalyzed by different CA isozymes were monitored spectrophotometrically, at 400 nm, with a Cary 3 instrument interfaced with an IBM-compatible PC. Solutions of substrate were prepared in DMSO; the substrate concentrations were 1 mM at 25 °C. A molar absorption coefficient of 400 M^{-1} cm^{-1} was used for the 4-nitrophenolate formed by hydrolysis in the conditions of the experiments (pH 7.5). Nonenzymatic hydrolysis rates were subtracted from the observed rates. The experiments were repeated three times at each inhibitor concentration. Stock solutions of the inhibitor (50 mM) were prepared and diluted up to 0.5 nM with DMSO. At least 8 different inhibitor concentrations have been used, ranging from 5 mM, 0.5 mM, 50 mM, 5 mM, 0.5 mM, 50 nM, 5 nM, 0.5 nM. Inhibitor and enzyme solutions were preincubated together for 15 min at r.t. prior to the assay study, to allow for the formation of the E-I complex. Enzyme concentrations were 1 ng/L for CA II [36]. Isoforms hCA IX has a low esterase activity compared to hCA II. However, we also obtained a good test condition by constantly adjusting the dosage of hCA IX enzyme.

5.6. MTT assay in vitro

Cell viability was evaluated using an MTT assay. Cancer cells were seeded into 96-well plates at a density of 5×10^4 cells per well and stabilized at 37 °C for 24 h. Compounds AAZ and **14a -14g** were added to each well at one concentration (0.1 mM), and then the cells were incubated for 72 h. The MTT solution (20 mL 5 mg/mL) was added to each well, and the cells were incubated for another 4 h. Formazan crystals were dissolved in 150 mL of DMSO. Cell viability was assessed by measuring the absorbance at 540 nm wavelength using a microplate reader (BioTek ELx800 USA).

Low oxygen conditions were acquired in a hypoxic workstation (Hypoxia Modular Incubator Chamber MIC-101, Billups-Rothenberg Inc, USA). The atmosphere in the chamber consisted of 0.5% O_2 (hypoxia), 5% CO_2, and residual N_2. Inparallel, normoxic (20% O_2) dishes were incubated in air with 5% CO_2.

5.7. Measurement of extracellular pH

Changes in pHe were assessed by using procedures published previously [37]. In brief, cells were plated and allowed to recover overnight. A standard volume of 3 mL of fresh media/dish was then added and cells were incubated in normoxia or hypoxia for 72 h. Care was taken to ensure that cultures grown in normoxia and hypoxia were subconfluent and contained similar cell numbers. Media was collected and pH was measured immediately by a digital pH meter.

5.8. Molecular docking simulations

The experimental crystallographic structure of CA IX complex was retrieved from the Protein Data Bank [38] (PDB: 3IAI [39]). The molecular model of the sulfonamide derivatives were built by Discovery Studio 3.5. Both the protein and the ligands were prepared by adding polar hydrogen atoms and partial charges with the assistance of AutoDockTools 1.5.6. AutoDock4Zn force field [40] was used to handle the zinc ion in the binding site. Grid points were increased to 60 at x, y, z axes. The number of Dock runs was increased to 20. All other parameters were kept as their default values [41].

Acknowledgments

This project was financially supported by National Natural Science Foundation of China (No. 81473087 and 81573292). Dr. Y. Liu wishes to express his thanks for the support by the Program for Liaoning Excellent Talents in University (LJQ2014110).

Appendix A. Supplementary data

The ^{1} H and ^{13}C NMR spectra of synthesized compounds are provided in supporting information.

Supplementary data related to this article can be found at http://dx.doi.org/10.1016/j.ejmech.2017.03.023.

References

[1] C.T. Supuran, How many carbonic anhydrase inhibition mechanisms exist? Enzyme Inhib. Med. Chem. 31 (2016) 345–360.
[2] (a) C.T. Supuran, Carbonic anhydrases: novel therapeutic applications for inhibitors and activators, Nat. Rev. Drug Discov. 7 (2008) 168–181;
(b) V.M. Krishnamurthy, G.K. Kaufman, A.R. Urbach, I. Gitlin, K.L. Gudiksen, D.B. Weibel, G.M. Whitesides, Carbonic anhydrase as a model for biophysical and physical organic studies of proteins and protein ligand binding, Chem. Rev. 108 (2008) 946–1051.
[3] C.T. Supuran, A. Scozzafava, Carbonic anhydrases as targets for medicinal chemistry, Bioorg. Med. Chem. 15 (2007) 4336–4350.
[4] (a) M.J. Smeulders, T.R. Barends, A. Pol, A. Scherer, M.H. Zandvoort, A. Udvarhelyi, A.F. Khadem, A. Menzel, J. Hermans, R.L. Shoeman, H.J. Wessels, L. Russ, I. Schlichting, M.S. Jetten, Evolution of a new enzyme for carbon disulphide conversion by an Acid other mophilic archaeon, Nature 478 (2011) 412–416;
(b) V. Alterio, A. Di Fiore, K. Ambrosio, C.T. Supuran, Multiple binding modes of inhibitors to carbonic anhydrases: how to design specific drugs targeting 15 different isoforms? Chem. Rev. 112 (2012) 4421–4468;
(c) C.T. Supuran, Carbonic anhydrases: novel therapeutic applications for inhibitors and activators, Nat. Rev. Drug Discov. 7 (2008) 168–181.
[5] (a) T. Ogawa, K. Noguchi, M. Saito, Y. Nagahata, H. Kato, A. Ohtaki, H. Nakayama, N. Dohmae, Y. Matsushita, M. Odaka, M. Yohda, H. Nyunoya, Y. Katayama, Carbonyl sulfide hydrolase from Thiobacillus thioparus strain THI115 is one of the β-carbonicanhydrase family enzymes, J. Am. Chem. Soc. 135 (2013) 3818–3825;
(b) D. Neri, C.T. Supuran, Interfering with pH regulation in tumoursas a therapeutic strategy, Nat. Rev. Drug Discov. 10 (2011) 767–777;
(c) K.S. Smith, C. Jakubzick, T.S. Whittam, J.G. Ferry, Carbonic anhydrase is an ancient enzyme widespread in prokaryotes, Proc. Natl. Acad. Sci. U. S. A. 96 (1999) 15184–15189;
(d) C.T. Supuran, Structure-based drug discovery of carbonic anhydrase inhibitors, J. Enzyme Inhib. Med. Chem. 27 (2012) 759–772.

[6] (a) N. Krall, F. Pretto, W. Decurtins, G.J.L. Bernardes, C.T. Supuran, D. Neri, A small-molecule drug conjugate for the treatment of carbonic anhydrase IX expressing tumors, Angew.Chem. Int. Ed. 53 (2014) 4231–4235;
(b) M. Aggarwal, C.D. Boone, B. Kondeti, Structural annotation of human carbonic anhydrases, J. Enzyme Inhib. Med. Chem. 28 (2013) 267–277;
(c) G. DeSimone, V. Alterio, C.T. Supuran, Exploiting the hydrophobic and hydrophilic binding sites for designing carbonic anhydrase inhibitors, Expert Opin. Drug Discov. 8 (2013) 793–810;
(d) E. Masini, F. Carta, A. Scozzafava, C.T. Supuran, Antiglaucoma carbonic anhydrase inhibitors: a patent review, Expert Opin. Ther. Pat. 23 (2013) 705–716;
(e) R.G. Gieling, C.A. Parker, N. Robertson, A.L. Harris, I.J. Stratford, K.J. Williams, Inhibition of carbonicanhydrase activity modifies the toxicity of doxorubicin and melphalanin tumour cells in vitro, J. Enzyme Inhib. Med. Chem. 28 (2013) 360–369.

[7] J. Chiche, J. Laferriere, E. Trottier, F. Dayan, N.M. Mazure, M.C. Brahimi-Horn, J. Pouyssegur, Hypoxia-inducible carbonic anhydrase IX and XII pro-mote tumor cell growth by counteracting acidosis through the regulation ofthe intracellular pH, Cancer Res. 69 (2009) 358–368.

[8] J. Chiche, M.C. Brahimi-Horn, J. Pouyssegur, Membrane-bound carbonic anhydrases are key pH regulators controlling tumor growth and cell migration, Adv. Enzyme. Regul. 50 (2010) 20–33.

[9] C.C. Wykoff, N.J. Beasley, P.H. Watson, K.J. Turner, J. Pastorek, A. Sibtain, G.D. Wilson, H. Turley, K.L. Talks, P.H. Maxwell, C.W. Pugh, P.J. Ratcliffe, A.L. Harris, Hypoxia-inducible expression of tumor-associated carbonic anhydrases, Cancer Res. 60 (2000) 7075–7083.

[10] P. Swietach, A. Harris, Regulation of tumor pH and the role of carbonic anhydrase 9, Cancer Metastasis Rev. 26 (2007) 299–310.

[11] J. Chiche, M. Brahimi-Horn, J. Pouysségur, Tumour hypoxia induces a metabolic shift causing acidosis: a common feature in cancer, J. Cell. Mol. Med. 14 (2010) 771–794.

[12] R.M. Zaguilan, E. Seftor, R. Seftor, Y. Chu, R. Gillies, M. Hendrix, Acidic pH enhances the invasive behavior of human melanoma cells, Clin. Exp. Metastasis 14 (1996) 176–186.

[13] A. Scozzafava, L. Menabuoni, F. Mincione, F. Briganti, G. Mincione, C.T. Supuran, Carbonic anhydrase inhibitors. Synthesis of water-soluble, topically effective, intraocular pressure-lowering aromatic/heterocyclic sulfonamides containing cationic or anionic moieties: is the tail more important than the ring? J. Med. Chem. 42 (1999) 2641–2650.

[14] C.T. Supuran, Carbonic anhydrases: from biomedical applications of the inhibitors and activators to biotechnologic use for CO_2 capture, J. Enzyme Inhib. Med. Chem. 28 (2013) 229–230.

[15] (a) C.T. Supuran, A. Scozzafava, Carbonic anhydrase inhibitors. Synthesis of water-soluble sulfonamides incorporating β-alanyl moieties, possessing long lasting-intraocular pressure lowering properties via the topical route, Eur. J. Med. Chem. 35 (2000) 309–321;
(b) Z. Wang, Y. Qin, P. Wang, H. Zhu, Sulfonamides containing coumarin moieties selectively and potently inhibit carbonic anhydrases II and IX: design, synthesis, inhibitory activity and 3D-QSAR analysis, Eur. J. Med. Chem. 66 (2013) 1–11.

[16] B.L. Wilkinson, L.F. Bornaghi, T.A. Houston, A. Innocenti, C.T. Supuran, S.A. Poulsen, A novel class of carbonic anhydrase Inhibitors: glycoconjugate benzene sulfonamides prepared by “Click-Tailing”, J. Med. Chem. 49 (2006) 6539–6548.

[17] B.L. Wilkinson, L.F. Bornaghi, T.A. Houston, A. Innocenti, D. Vullo, C.T. Supuran, S.A. Poulsen, Inhibition of membrane-associated carbonic anhydrase isozymes IX, XII and XIV with a library of glycoconjugate benzenesulfonamides, Bioorg. Med. Chem. Lett. 17 (2007) 987–992.

[18] B.L. Wilkinson, L.F. Bornaghi, T.A. Houston, A. Innocenti, D. Vullo, C.T. Supuran, S.A. Poulsen, Carbonic anhydrase Inhibitors: inhibition of isozymes I, II, and IX with triazole-linked O-Glycosides of benzene sulfonamides, J. Med. Chem. 50 (2007) 1651–1657.

[19] M. Aggarwal, B. Kondeti, R. McKenna, Insights towards sulfonamide drug specificity in alpha carbonic anhydrases, Bioorg. Med. Chem. 21 (2013) 1526–1533.

[20] C.T. Supuran, S.A. Poulsen, Carbonic anhydrase inhibitors with dual-tail moieties to match the hydrophobic and hydrophilic halves of the carbonic anhydrase active site, J. Med. Chem. 58 (2015) 1494–1501.

[21] (a) C.T. Supuran, A. Scozzafava, Carbonic anhydrase inhibitors and their therapeutic potential, Exp. Opin. Ther. Pat. 10 (2000) 575–600;
(b) M. Krasavin, M. Korsakov, M. Dorogov, T. Tuccinardi, N. Dedeogl, C.T. Supuran, Probing the ‘bipolar’ nature of the carbonic anhydrase active site: aromatic sulfonamides containing 1,3-oxazol-5-yl moiety as picomolar inhibitors of cytosolic CA I and CA II isoforms, Eur. J. Med. Chem. 101 (2015) 334–347.

[22] C.T. Supuran, Dithiocarbamates strongly inhibit carbonic anhydrases and show antiglaucoma action in vivo, J. Med. Chem. 55 (2012) 1721–1730.

[23] T. Tuccinardi, S. Bertini, C.T. Supuran, Salicylaldoxime derivatives as new leads for the development of carbonic anhydrase inhibitors, Bioorg. Med. Chem. 21 (2013) 1511–1515.

[24] A. Maresca, G. Akyuz, S.M. Osman, Z. AlOthman, C.T. Supuran, Inhibition of mammalian carbonic anhydrase isoforms I-XIV with a series of phenolic acid esters, Bioorg. Med. Chem. 23 (2015) 7181–7188.

[25] I. Nehls, Koenigs–Knorr reaction of fusel alcohols with methyl (1-bromo-2, 3, 4-tri-O-acetyl-α-D-glucopyranosid)uronate leading to the protected alkyl-glucuronides—crystal structures and high resolution ^{1}H and ^{13}C NMR data, Carbohydr. Res. 352 (2012) 186–190.

[26] G. Wei, S. Cui, W. Luan, S. Wang, Z. Hou, Y. Liu, Y. Liu, M. Cheng, Natural product-based design, synthesis and biological evaluation of Albiziabioside A derivatives that selectively induce HCT116 cell death, Eur. J. Med. Chem. 113 (2016) 92–101.

[27] A. Grandane, M. Tanc, L.D.C. Mannelli, F. Carta, C. Ghelardini, R. Alubovskis, C.T. Supuran, 6-Substituted sulfocoumarins are selective carbonic anhdydrase IX and XII inhibitors with significant cytotoxicity against colorectal cancer cells, J. Med. Chem. 58 (2015) 3975–3983.

[28] J.C. Morris, J. Chiche, C. Grellier, M. Lopez, L.F. Bornaghi, A. Maresca, C.T. Supuran, J. Pouyss, S.A. Poulsen, Targeting hypoxic tumor cell viability with carbohydrate-based carbonic anhydrase IX and XII inhibitors, J. Med. Chem. 54 (2011) 6905–6918.

[29] R.G. Gieling, M. Babur, L. Mamnani, N. Burrows, B.A. Telfer, F. Carta, J.Y. Winum, A. Scozzafava, C.T. Supuran, K.J. Williams, Antimetastatic effect of sulfamate carbonic anhydrase IX inhibitors in breast carcinoma xenografts, J. Med. Chem. 55 (2012) 5591–5600.

[30] S.K. Parks, J. Chiche, J. Pouyssegur, pH control mechanisms of tumor survival and growth, J. Cell Physiol. 226 (2011) 299–308.

[31] J. Chiche, J. Laferriere, E. Trottier, F. Dayan, N.M. Mazure, Hypoxia-inducible carbonic anhydrase IX and XII promote tumor cell growth by counteracting acidosis through the regulation of the intracellular pH, Cancer Res. 69 (2009) 358–368.

[32] S. Pastorekova, P.J. Ratcliffe, J. Pastorek, Molecular mechanisms of carbonic anhydrase IX-mediated pH regulation under hypoxia, BJU Int. 101 (2008) 8–15.

[33] E. Svastova, A. Hulikova, M. Rafajova, A. Gibadulinova, A. Casini, Hypoxia activates the capacity of tumor-associated carbonic anhydrase IX to acidify extracellular pH, FEBS Lett. 577 (2004) 439–445.

[34] L. Dubois, K. Douma, C.T. Supuran, R.K. Chiu, S. Pastorekova, A. Scozzafava, B.G. Wouters, P. Lambin, Imaging the hypoxia surrogate marker CA IX requires expression and catalytic activity for binding fluorescent sulfonamide inhibitors, Radiother. Oncol. 83 (2007) 367–373.

[35] J.A. Verpoorte, S. Mehta, J.T. Edsall, Anhydrases B and C Esterase activities of human carbonic enzymology, J. Biol. Chem. 242 (1967) 4221–4229.

[36] E. Truppo, C.T. Supuran, A. Sandomenico, D. Vullo, A. Innocenti, Carbonic anhydrase VII is glutathionylated without loss of catalytic activity and affinity for sulfonamide inhibitors, Bioorg. Med. Chem. Lett. 22 (2012) 1560–1564.

[37] A. Cecchi, A. Hulikova, J. Pastorek, S. Pastorekova, A. Scozzafava, J.Y. Winum, Carbonic anhydrase inhibitors. Design of fluorescent sulfonamides as probes of tumor-associated carbonic anhydrase IX that inhibit isozyme IX-mediated acidification of hypoxic tumors, J. Med. Chem. 48 (2005) 4834–4841.

[38] H.M. Berman, J. Westbrook, Z. Feng, G. Gilliland, T.N. Bhat, H. Weissig, I.N. Shindyalov, P.E. Bourne, Protein Data Bank Nucleic Acids Res. 28 (2000) 235–242.

[39] V. Alterio, M. Hilvo, A. Di Fiore, C.T. Supuran, P. Pan, S. Parkkila, A. Scaloni, J. Pastorek, S. Pastorekova, C. Pedone, A. Scozzafava, S.M. Monti, G. De Simone, Crystal structure of the catalytic domain of the tumor-associated human carbonic anhydrase IX, PNAS 106 (2009) 16233–16238.

[40] D. Santos-Martins, S. Forli, M. João Ramos, A.J. Olson, AutoDock4Zn: an improved AutoDock force field for small-molecule docking to zinc metalloproteins, J. Chem. Inf. Mod. 54 (2014) 2371–2379.

[41] G.M. Morris, R. Huey, W. Lindstrom, M.F. Sanner, R.K. Belew, D.S. Goodsell, A.J. Olson, Autodock4 and AutoDockTools4: automated docking with selective receptor flexiblity, J. Comput. Chem. 16 (2009) 2785–2791.